Computer simulation of endlinked elastomers. I. Trifunctional networks cured in the bulk

YuKwan Leung and B. E. Eichinger

Citation: J. Chem. Phys. **80**, 3877 (1984); doi: 10.1063/1.447169
View online: http://dx.doi.org/10.1063/1.447169
View Table of Contents: http://jcp.aip.org/resource/1/JCPSA6/v80/i8
Published by the American Institute of Physics.

Computer simulation of end-linked elastomers. I. Trifunctional networks cured in the bulk[a)]

Yu-Kwan Leung
Department of Applied Science, Hong Kong Polytechnic, Hung Hom, Hong Kong
B. E. Eichinger
Department of Chemistry BG-10, University of Washington, Seattle, Washington 98195

(Received 30 September 1983; accepted 6 January 1984)

The end linking of difunctional poly(dimethylsiloxane) with trifunctional cross linkers in the bulk has been simulated with a computer. A random array of primary chains with a Gaussian end-to-end distribution is generated in an image container on the computer. By joining chain ends at nearby junctions, inter- and intramolecular reactions occur in all species, allowing formation of cyclic structures of any size. At high extents of reaction, the sol components extracted from the spanning forest thus constructed consist of a substantial amount of cycles such as cyclic dimers. The effect of intramolecular reaction increases the extent of reaction by several percent for molecular weights in the range of thousands. Structural statistics of various types of network imperfections and the cycle ranks of the networks are reported. The gels obtained at complete conversions contain loop defects, their populations increasing with lower molecular weights of the prepolymers. The elastic activities of nonstoichiometric systems are compared and discussed.

I. INTRODUCTION

An accurate description of gelation processes requires consideration of the effect of intramolecular reactions which must occur during a nonlinear polymerization. Recent efforts to account for cyclization in stepwise polyreactions, which extend the gelation statistics of Flory[1] and Stockmayer,[2] include modified cascade theory[3] and rate theory.[4] In addition to results presented in analytical form, computer simulations of gelation by Monte Carlo methods[5] have also attracted considerable attention.

Simulations of network formation on the computer have developed along two lines: the percolation method[6] and the kinetic method.[7,8] In the percolation method, the f-functional monomers occupy sites of a d-dimensional lattice. This model, which is analogous to a solid-state polymerization, would inevitably produce a network with abundant short circuits formed from the smallest cycle on the lattice. Simulation of a liquid-phase polymerization by a crystallographic approach results in an overestimation of the proportion of intramolecular reactions. At the other extreme, branching theory[1,9] totally suppresses cyclization. The difference between these approaches is reflected in their predictions of the critical extent of reaction p_c at the gel point. In a RA_f self-polymerization, "bond" percolation on a three-dimensional tetrahedral lattice[10] gives a gel point at $p_c = 0.390$, whereas the critical extent of reaction for a treelike model[1] is 0.333, that is $1/(f-1)$. The experimental gel point is expected to fall between the two calculated values. "Site" percolation yields an even higher p_c value because in the site problem, all neighboring elements in the same cluster are implicitly linked to each other. Thus, the reaction must be carried further to reach the critical state. For a tetrahedral lattice, the site percolation places the critical extent of reaction at 0.43.[10] Percolation on lattices is nonetheless valuable for the study of critical behavior near the transition threshold within the framework of renormalization group theory.

In the kinetic scheme, specific reaction routes have to be written down to include the formation of cyclic as well as acyclic molecules. This procedure requires a long list of rate equations and a great deal of computer coding.[3,4] For the early stages of the reaction, the rate theory depicts both the exact size distributions and the probabilities for intramolecular reactions.[4]

Beyond the gel point, the problem of gel–sol distributions is complicated by the strong competition between intramolecular and intermolecular reactions. However, in most studies, it has been assumed that the sol molecules are acyclic.[1,8,9] As noted above, the postulate of treelike sols may lead to distorted distributions and inaccurate gelation conditions, and one must expect that these inaccuracies will persist beyond the gel point. Shortcomings in the kinetic approach, where systems are composed of functional groups that are selected at random without spatial constraint, and in the percolation method where an ordered arrangement is assured, has led us to formulate a different method. In our model, a more realistic approach is adopted by utilizing the computer to simulate a random array of molecules with a Gaussian end-to-end distribution.[11] The growth of the polymeric molecules is accomplished by an end-linking process.[12] Since there is no discrimination against any particular type of reaction, rings of any size can be formed in all species. The first article of this series deals with the gel–sol distributions for the $A_2 + B_3$ system. The program can be adapted to simulate other types of polymerization and to cover the entire range of the polymerization process. We are presently studying the critical phenomenon of gelation for various types of nonlinear polymerizations. The results of those investigations will be published in due time.

II. ALGORITHM

Difunctional prepolymers (A_2) having n skeletal bonds were copolymerized with cross-linking units with functionality f (B_f). The chain ends and cross linkers are assumed to be randomly distributed in the image reaction box. It is an accu-

[a)] This work performed at the University of Washington.

 0021-9606/84/083877-08$02.10

rate approximation to make the liquid structure a random distribution for prepolymers of sufficient high molecular weight or for dilute concentrations of reactive groups, and it is reasonable to do the same for more modest molecular weights. A number N_p of A_2 prepolymers were distributed randomly in a cubical box whose length L is determined from

$$L = \left[\frac{n M_0 N_p}{\rho N_a}\right]^{1/3}, \tag{1}$$

where M_0 is the average molecular weight of one bond unit, ρ is the density of the network, and N_a is Avogadro's number. The distribution of end-to-end distances of the primary chains assumes a three-dimensional Gaussian function with a one-dimensional variance[13] σ^2 given by

$$\sigma^2 = C_n n l^2/3, \tag{2}$$

where l is the length of one backbone bond and C_n is the characteristic ratio.[14] The number of randomly distributed cross-linkers N_c is

$$N_c = 2rN_p/f. \tag{3}$$

The stoichiometric ratio r is defined as the ratio of the numbers of B to A functional groups.

The growth of the molecules proceeded by joining available neighboring reactive groups. Formation of an –AB– bond took place in the order of increasing r_{AB}, the distance between functional groups A and B. Discrete molecules are treated as graphs where a vertex is defined as a condensed point of a graph and the degree of a vertex equals the number of primary chains attached to it. Reaction between the chosen A and B points occurred provided that the following conditions were satisfied: (1) the A group was unreacted, (2) the degree of the cross linker to which the B group belonged was less than the maximum allowable number f, and (3) the corresponding r_{AB} was less than the set distance parameter d. Thus, the extent of reaction of A functional groups P_A is controlled by the value d.

During the end-linking process, the details of connectivity were recorded. The parity of the chain end, which indicates whether it has reacted or not, is designated as PAR. The indices of ends to which the connections were made through the shared cross linker is called the connecting index. By keeping track of the degree and the connecting index of the visited ends, designated as DEG and IND respectively, a connectivity table describing the assemblage of graphs was obtained. Finally, the connected components were sorted out by using the spanning-tree program SPANFO written by Nijenhuis and Wilf.[15]

The programming pattern follows:

(1) Index A functional groups by I. The first ends of the primary chains are represented by $I = 2N - 1$ and the second ends by $I = 2N$ for $1 \leqslant N \leqslant N_p$.

(2) Generate N_p uniformly distributed random numbers between $(0,L)$ in each of three dimensions[16] as the coordinates of odd I.

(3) Generate $3N_p$ random numbers with a Gaussian distribution with variance given by Eq. (2).[16] The coordinates of the $(2N)$th end are obtained by adding these Gaussian numbers to the coordinates stored for the $(2N-1)$th end.

(4) Index f-functional cross-linking units by J: $1 \leqslant J \leqslant N_c$.

(5) Locate J with uniformly distributed random numbers generated as in (2).

(6) Divide the L^3 cube into $7 \times 7 \times 7$ regions and assign I and J to the appropriate region.

(7) Start from region (1,1,1).

(8) Calculate r_{IJ} between I and J for all J belonging to region (K,L,M) and for all I that lie in the same region and in neighboring regions. If $r_{IJ} > d$, reject; otherwise, put r_{IJ} into the distance set.

(9) Arrange r_{IJ} in ascending order.

(10) Initiate PAR(I)←0 for $I = 1,2N_p$; DEG(J)←0 and IND(J)←0 for $J = 1,N_c$.

(11) Select (I,J) pairs consecutively, beginning with the smallest r_{IJ}. If PAR(I) = 0 and DEG(J) $< f$, then set PAR(J)←1 and DEG(J)←DEG(J) + 1. Otherwise, skip.

(12) Change the connecting index of the vertex involved: check if IND(J) = 0; if so, set IND(J)←I; else IND(J)←MINO[I,IND(J)].

(13) Repeat steps (11) and (12) until all elements in the r_{IJ} set are read.

(14) Sweep bond formation region by region by repeating steps (8) to (13).

(15) Assign new indices NEW(I) for ends of primary chains by doing NEW(I)←IND(J) if the I th end is attached to the Jth cross linker. If the Ith end is unreacted, NEW(I)←I.

(16) Renumber the two ends of the N th primary chain as follows:

END(1,N)←MINO(NEW($2N-1$),$2N-1$)

and

END(2,N)←MINO(NEW($2N$),$2N$) for $1 \leqslant N \leqslant N_p$.

(17) Given the array END(L,M) as input, find the connected components by the SPANFO subroutine.[15]

(18) Identify graph structure of the sol molecules and the dangling ends of the gel component by examining the degrees of the vertices.

At high conversions, only one large particle was observed and was identified as the gel. The remaining species are sol molecules, each of which was found to contain fewer than 20 chains. The smallest loop consists of only one primary chain. The structure of the sol molecules can be recognized by referring to the set of the degrees assigned to its vertices and the number of one-chain loops formed.[12] An exposition of the sol molecules for the trifunctional system is given in Table I. Dangling ends of the molecules are those vertices whose degree equals one. Local structure in the gel can be identified by inspecting the degree of the junction that has an unconnected end attached to it.

TABLE I. Sol constituents for end-linked trifunctional reaction.[a]

No.	Graph	Weight %[b]	No.	Graph	Weight %[b]
1		2.40 (0.09)	6		0.61 (0.10)
2		0.075 (0.013)	7		0.022 (0.03)
3		0.065 (0.034)	8		0.0075 (0.01)
4		0.79 (0.01)	9		0.08 (0.02)
5		0.01 (0.01)	10		0.03 (0.06)

[a] $n = 50$ and $P_A = 0.897$.

[b] Standard deviations are given in parentheses.

III. RESULTS

Simulations were done for trifunctional end-linked poly(dimethylsiloxane) elastomers.[17,18] Values of the PDMS parameters are: $M_0 = 37$ g/mol, $C_n = 6.3$, $l = 1.64$ Å, and $\rho = 0.97$ g/cm^3.[14] Computations on systems of different size were performed to investigate the effect of finite sample size.[11] No consistent trend due to an edge effect was observed if more than 5000 primary chains per configuration were sampled. The speed of convergence with size is consistent with results obtained by other methods.[8,19] Results averaging over four different configurations of 10 000 A_2 molecules each are reported for all following calculations. The errors ascribable to an edge effect are estimated to be no greater than the standard deviations due to statistical fluctuations. The latter are roughly 10% of the calculated quantities reported below. Given these observations, it is concluded that finite systems of this size are essentially indistinguishable from the limiting behavior for an infinite system. Exact stoichiometric balance was maintained for all reactions unless otherwise stated.

A. Molecular constituents of the sol

Representative sol compositions obtained by polymerizing primary PDMS molecules having 50 Si–O bonds are tabulated in Table I. The reaction proceeded to 89.7% extent of reaction, yielding a sol weight fraction of 0.051. Figure 1 shows a histogram of the weight fraction of x-mer (W_x) for this particular degree of conversion. Here, the shaded bars represent the weight fractions W_x of cyclics, and the open bars are those of the treelike molecules. The proportion of

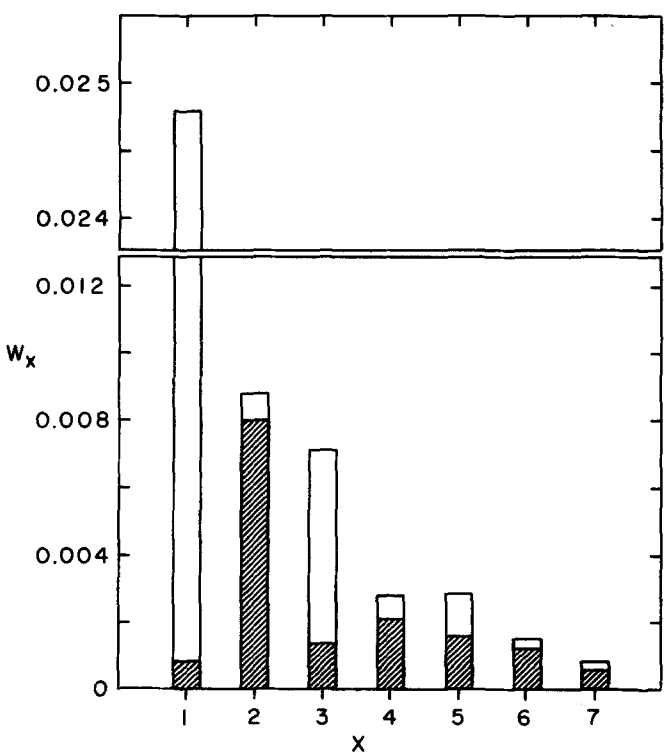

FIG. 1. Histogram showing weight fractions of finite species obtained from polymerizing primary chains having 50 skeletal bonds to $P_A = 0.897$. The shaded bars represent weight fractions of cyclic x-mers, whereas the open bars indicate those of the acyclics.

cyclics in each class of x-mer varies depending upon the availability of reactive B groups to which ring closure can be made. Features of the constituents of the sol are summarized as follows:

(1) The most abundant molecule is the linear monomer which constitutes ~50% of the weight of the sol.

(2) There are three types of dimer: the linear, the tadpole, and the double edge, present in the ratio 13:80:1. The tadpole dimer containing only one reactive group at the tail is a relatively stable species because it has less chance to be absorbed by the gigantic gel particle than do the other dimers.

(3) The branched trimer, which requires only one cross-linking agent, is more abundant than other types of trimer which take up two cross linkers.

(4) The loop trimer outnumbers the double-edge trimer by a 3:1 margin (see structures 7 and 8 in Table I).

(5) Saturated molecules, such as the dumbbell (structure 9) and the fanblade (structure 10), are found in relatively large amounts because they are inert.

(6) Most large species contain ring structures.

These findings can be understood in terms of reaction statistics. Imagine that cyclic trimers are formed from the linear counterpart via a one-step closure reaction: if the free ends of the linear trimer attack its nearest junction, a tadpole trimer is produced, whereas a double-edge trimer is obtained if the attachment is made at the second nearest junction. The probability of ring formation is weighted by the factor $n^{-3/2}$ derived from Gaussian statistics. The ratio of populations between the loop trimer and the double-edge trimer is therefore

$$2n^{-3/2}/2(2n)^{-3/2} = 2^{3/2} = 2.83;$$

the factor 2 is the number of routes leading to the cyclic structure from the starting graph. The experimental value of this ratio, averaged over 12 systems covering a wide range of extents of reaction and chain lengths, is found to be 2.4 with a standard deviation of 1.0. The large standard deviation is the consequence of sampling very few molecules in each system, e.g., the number of cyclic trimers is less than 15 in each sample. From the numerical values given in Table I, the ratio is 3.0 for this particular system. The close agreement with the predicted value confirms that results obtained are in accordance with the Gaussian distribution assumed by the primary chains.

The probabilities for occurrence of the tadpole dimer and the double-edge dimer are $(1 - P_A)P_A^3 P_{3C} n^{-3/2}$ and $P_A^4 P_{2C}^2 (2n)^{-3/2}$, respectively, where P_{iC} is the probability of finding a cross linker of degree i. The ratio between these two is therefore given by $2^{3/2}\,(1 - P_A)P_{3C}/P_A P_{2C}^2$. Given the P_{2C} and P_{3C} values to be 0.0555 and 0.844, respectively, from the computer simulation, the number of tadpole dimers is ~90 times that of double-edge dimers, which is close to the value of 80 found for this particular system.

B. Variations of graph populations with conversion and chain length

In Figures 2 and 3, the mole fractions N_g of selected graphs are plotted against the extents of reaction for differ-

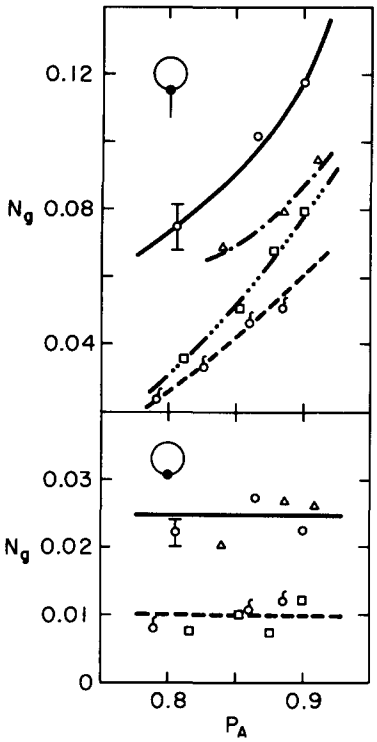

FIG. 2. Mole fractions of tadpole dimer and cyclic monomer. MW = 1850 (○), 4700 (△), 18 500 (□), and 32 900 (σ).

ent molecular weights of the end-reactive oligomer. The results for MW = 1850, 4700, 18 500, and 32 900 are given by the *circles*, *triangles*, *squares*, and *apples*, respectively. The curves in Fig. 2 show broadly the expected trend of N_g with chain lengths of the primary chains in that the chance of forming a loop increases as chain length decreases. Standard deviations, indicated by the bar located at data points for MW = 1850 and $P_A = 0.809$, increases with higher extents of reaction as fewer sol molecules are sampled. The relationship between loop population and chain length will be discussed in more detail in the following paper.[20]

The influence of molecular weight on acyclic species depends upon the tendency to form ring structures. It can be seen in Fig. 3 that the proportion of branched trimer seems to be independent of molecular weight, whereas the number of linear dimers shows a slight decrease with smaller molecular weights. This can be rationalized by noting that the ends of the linear dimer can react with its midchain reactive B group to form a tadpole but the chance of converting a trimer from the branched structure to one containing a double edge is reduced by a factor proportional to the probability of finding a free cross linker, which is rare at high conversions.

The mole fractions of acyclic species decrease monotonically with the extents of reaction as expected. For the cyclics, the pattern will be more complicated. Since the tadpole dimer is a quasistable structure, its rate of disappearance is less than that of other sol molecules, which makes its relative population increase with higher conversions. However, the mole fraction must drop to zero as the reaction nears completion, since the reactive tail must eventually become either a part of the gel or a constituent of a truly inert sol molecule.

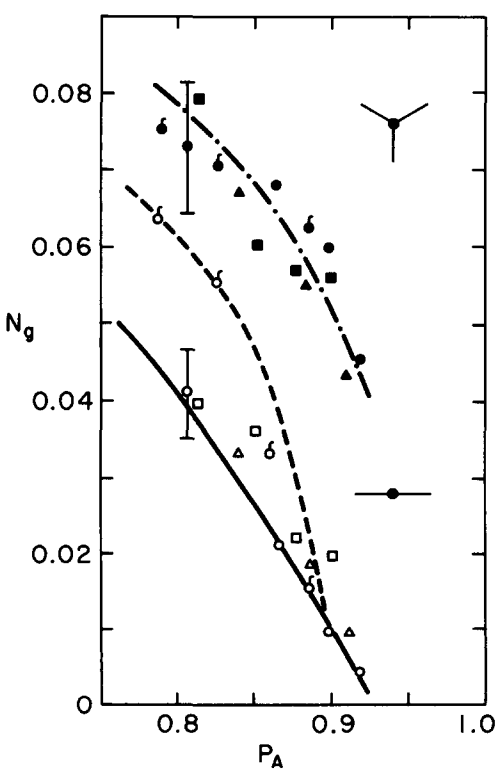

FIG. 3. Mole fractions of branched trimer (filled symbol) and linear dimer (open symbol). Symbols correspond to those in Fig. 2.

C. Sol fraction

The sol fraction contains reactive cyclics, inert material, and low molecular weight trees. To obtain an exact relation between the amount of sol and the extent of reaction of the polymerization, it is necessary to take into account the effect of intramolecular reaction leading to the formation of cyclics.[21] The program described here allows cyclics in the sol without restriction beyond those imposed by the chosen model of the liquidlike structure and the kinetics. Results for the weight fractions w_s of soluble material that were generated for trifunctional networks are presented in Table II. For comparison, sol fractions w_s' derived by branching theory,[9] which assumes that only treelike molecules exist in the sol,

TABLE II. Sol fractions for $A_2 + B_3$ systems.

MW	r	P_A	w_s	$w_s'^a$
1 850	1.0	0.809	0.172	0.152
		0.864	0.083	0.054
		0.897	0.051	0.022
		0.920	0.037	0.013
4 700	1.0	0.883	0.051	0.036
		0.910	0.032	0.018
18 500	1.0	0.851	0.069	0.070
		0.877	0.047	0.045
		0.897	0.033	0.024
1 850	0.8	0.766	0.162	0.110
		0.778	0.145	0.091
		0.785	0.136	0.080
1 850	1.2	0.872	0.130	0.150
		0.915	0.062	0.062
		0.942	0.035	0.030

[a] Reference 9.

are entered into the last column of Table II. It can be seen that the differences between w_s and w_s' increase with shorter chain lengths and higher extents of reaction as anticipated. The trend is consistent with the proportion of intramolecular reaction as discussed in Sec. III B. For MW = 4700, a sol fraction yield of 0.03 requires that the reaction be carried to 92.5% completion, which is higher than the value of 89.9% predicted by the branching theory. To achieve a cross-linking efficiency of 95% reported by Mark and co-workers,[17] the corresponding sol will be 2% of the total weight. Since the sol quantities involved are very small and are determined[18] after subtraction of the estimated amount of unreative cyclic materials present in the starting PDMS oligomers, the inherent reliability of extents of reaction derived from sol fractions depends largely upon the efficiency of reclamation of the sol and on the accurate correction for the "purity" of the prepolymers.

For systems composed of a large excess of cross linker, e.g., $r = 1.2$ in Table II, the treelike model can describe the P_A vs w_s relationship adequately. On the contrary, for $r < 1$, the largest deviation between w_s and w_s' occurs at complete consumption of the cross-linking groups.

In our model, a residue of sol comprised of inert materials, such as the dumbbell and the fanblade always remains at complete conversion. For example, ~0.5% of the prepolymer finds its way to small, inert molecules in the polymerization of primary chains having 50 skeletal bonds. It must be noted, however, that the inextractable cyclics that are permanently incarcerated by interpenetration with a real network are not distinguished in these simulations. To identify such incarcerated cyclic sol molecules would require simulations with chain trajectories included.

D. Network imperfections

To eliminate any influence attributable to an edge effect, only the interior portion of the generated networks were considered; the interior gel is the assembly of vertices which are at least a distance d inside the wall of the box. Our program can identify specific short, circuitous paths, such as one-chain loops, two-chain loops, double-edge circuits, and various types of dangling ends. The population of such network irregularities η is expressed in terms of the number of fragments of a particular type that occur, relative to the number of primary chains incorporated in the gel.

The population of one-chain loops is plotted against the extent of reaction at different molecular weights in Fig. 4. One such configuration is made by four primary chains. Symbols used are the same as those of Figure 2. The remainder of the network is indicated by jagged lines. It can be seen that the population of one-chain loops increases with the extent of reaction. A sizable percentage of one-chain loops, varying from 1% to 3% depending on MW, remains at complete conversion and contributes defects to the networks.

The probability of forming two-chain loops and double-edged circuits in the gel is very small. Our results show that the ratio of one-chain loops to two-chain loops to double-edged circuits at $P_A = 0.809$ is 1:0.045:0.062 for $n = 50$. This ratio changes to 1:0.019:0.093 as the reaction proceeds to 90.0% conversion. From these observations, it seems that

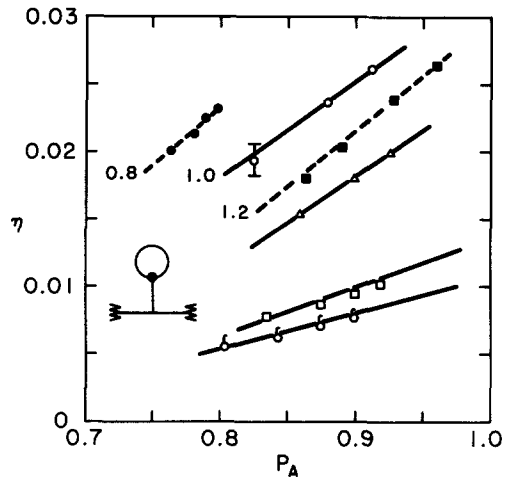

FIG. 4. Plots of dangling loop population vs the extent of reaction at different MW (same symbols as in Fig. 2). Broken lines represent nonstoichiometric systems with r values indicated.

the share of defects arising from reactions between two or more functions attached to the same two primary chains does not exceed ~10% of the one-chain population, regardless of the extent of reaction. Circuit structures involving three or more primary chains in the gel were not identified by the program.

For trifunctional networks, there are two types of dangling end configurations, namely, the "I" type and the "Y" type (see Fig. 5). Their populations are observed to be molecular weight independent. This implies that the competition between loops and these branched structures is negligible. The Y type vanishes faster with increasing extent of reaction

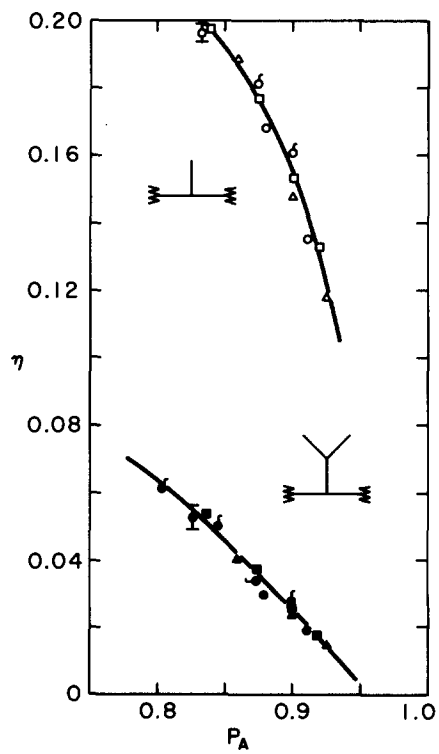

FIG. 5. Plots of the I and Y free end populations in the gel (symbols same as in Fig. 2).

because it is converted into the I type when one of its unattached ends joins with another part of the network.

The elastic free energy for a phantom network is proportional to the cycle rank ξ of the network,[22] which is the number of cuts required to reduce the network to a tree.[23] For a macroscopic network consisting of ν chains and μ junctions,

$$\xi = \nu - \mu. \tag{4}$$

To evaluate this quantity, we adopt the notion that an effective junction is a vertex of a graph whose degree is greater than one, and effective chains are bounded by effective junctions.[24] The counting of dangling ends is somewhat arbitrary. We have chosen not to count the chain forming the loop whereas the junction to which the loop is attached is counted. In this way, the configuration depicted in Fig. 4 contributes one independent circuit relevant to elastic activity. The cycle rank per chain (ξ/ν) for various networks prepared from primary chains having 50 skeletal bonds are presented as the solid curves in Fig. 6. The values obtained at very high extents of reaction exhibit the influence of the imperfections discussed above.

An expression describing the cycle rank of an imperfect trifunctional network was derived by Queslel and Mark.[25] They assume that the gel is devoid of short circuitous paths and that the probability of finding a cross linker with degree less than two is negligible. It follows that the quantity ξ/ν for a trifunctional stoichiometric ($r = 1.0$) system is

$$\xi/\nu = 1 - 2/3P_A. \tag{5}$$

The dashed curve shown in Fig. 6 is drawn according to Eq. (5). The departure from the computer data, the solid curve labeled $r = 1.0$, increases as P_A decreases from unity. This is due to the increased concentration of unsaturated cross linkers. The discrepancy at $P_A = 1.00$ arises from loop defects in the gel. For a perfect network, the cycle rank per chain is $1 - 2/f$. Network imperfections contributed by one-

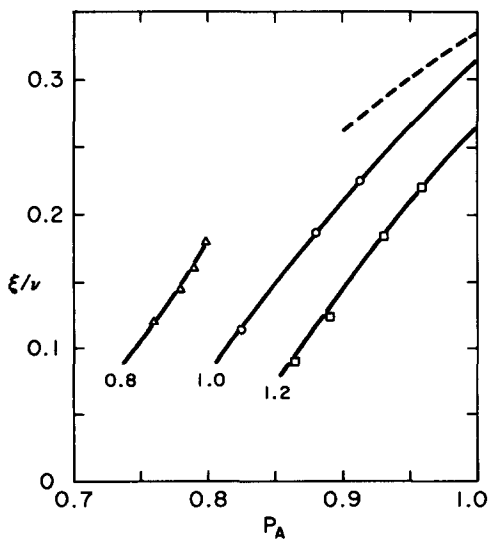

FIG. 6. Dependence of the cycle rank per chain for trifunctional end-linked PDMS networks ($n = 50$). Solid curves represent results obtained from this simulation at different values of the stoichiometric ratio r. Broken curve is drawn according to Eq. (5) for $r = 1.0$.

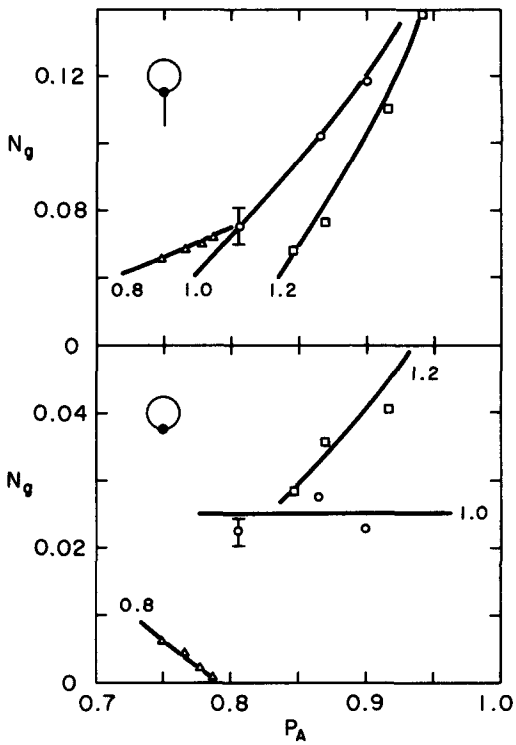

FIG. 7. Dependence of the mole fractions of tadpole and cyclic monomer upon the extent of reaction for different stoichiometric ratios: $r = 0.8$ (△), 1.0 (○), and 1.2 (□).

chain loops reduce the cycle rank per chain by an amount

$$\Delta(\xi/\nu) = -W_l, \tag{6}$$

where W_l is the weight fraction of primary chains that react

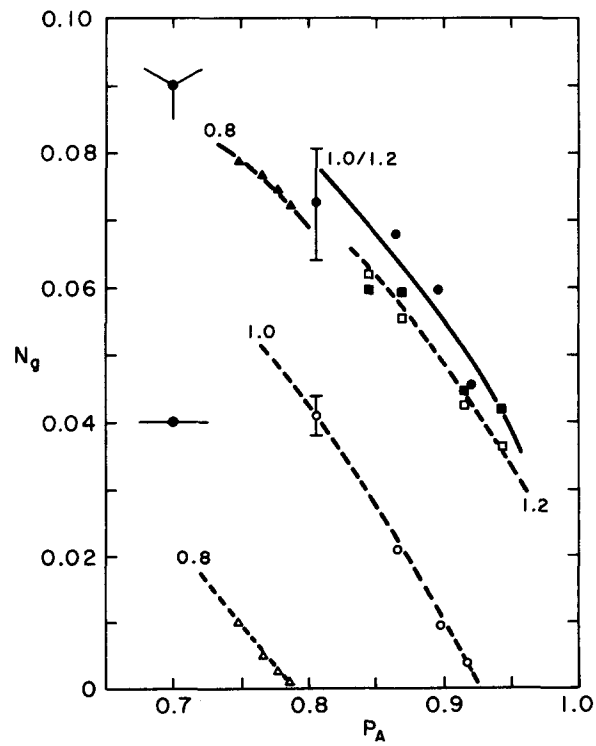

FIG. 8. Plots of the mole fractions N_g of branched trimer and linear dimer for different stoichiometric systems with r values indicated. The solid and the broken curves represent the N_g of branched trimer and linear dimer, respectively.

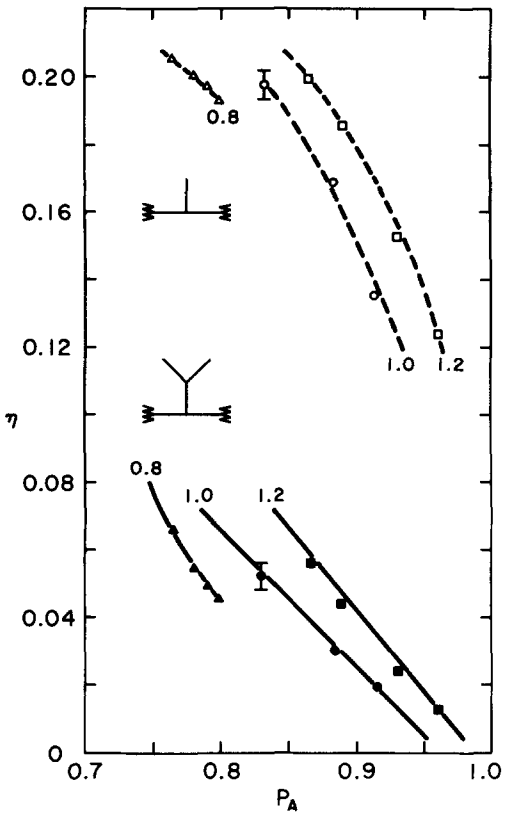

FIG. 9. Dependence of the η vs the extent of reaction at different r for the I and the Y dangling ends.

to form loops. The difference between ξ/ν for a perfect network (1/3) and that obtained by extrapolation of these data to complete conversion is ~ 0.02 for $n = 50$. This agrees reasonably well with the η value of ~ 0.03 obtained from Fig. 4 for the similar system, considering that both are long extrapolations. Dušek and Vojta[26] calculated the number of elastically inactive cycles in the gel by the spanning-tree approximation of the cascade theory. For elastomers cured in the bulk, the fraction of prepolymers forming the elastically inactive cycles is $\sim 2\%$, which agrees well with the W_l values obtained from this work.

E. Nonstoichiometric systems

Figures 7 and 8 show the mole fractions of tadpoles, cyclic monomers, branched trimers, and linear dimers for systems with different stoichiometric ratios. Results are represented by *triangles* ($r = 0.8$), *circles* ($r = 1.0$), and *squares* ($r = 1.2$). The mole fractions of cyclic monomer and linear dimer increase with the percentage of cross linker. This can be attributed to the enhanced opportunity for the linear monomer, which is the most abundant species, to capture an excess cross-linking unit to form either a cyclic monomer or a linear dimer. Concommitantly, the slope of the N_g curve (Fig. 7) for the cyclics increases as more cross-linkers are present. For cyclic monomer, an inversion of the sign of the slope from a negative value to a positive value is obtained. When the cross-linking agent is in short supply, the residual reactive B group attached onto the cyclic monomer will sooner or later be consumed and this results in the disappearance of the cyclic monomer. The reverse is true for systems which contain an excess of cross-linking units.

Variations of the population of loops and dangling ends in the gel with different r values are shown in Figs. 4 and 9. More unattached ends are found if the numbers of the respective functional groups are not balanced. In the presence of excess cross linker, the ends of the dangling primary chain are "reacted," or if the cross-linking agent is insufficient, they are "unreacted" ends. Network imperfections are represented by the pattern of cycle ranks depicted in Fig. 6. It is obvious that the most perfect networks are obtained when the stoichiometry is balanced. Therefore, the observation that maximal shear moduli are obtained for networks prepared with r a little larger than unity cannot be attributed to the perfection of the networks.[27] We obtain similar results for tetrafunctional networks.[20]

IV. CONCLUSION

Simulations of the end-linking process reported here illustrate the influence of intramolecular reactions on gel–sol distributions. The nature of ring formation is twofold. For the sol fraction, cyclic molecules such as the tadpole are present in substantial amounts at high extents of reaction, and the fraction of intramolecular reactions increases steadily with higher conversions. Neglect of this effect, as is done in theories that only count trees, would underestimate the extent of reaction by several percent. In the gel component, loop defects, such as one-chain loops and small circuits, are formed as the result of short-ranged intramolecular reactions. These defects do not vanish at complete conversion, and they reduce the cycle rank in proportion to the number of primary chains reacting to form loops. Networks made from very long primary chains should approach perfect structures with no loop defects, but then problems associated with slow diffusion for very high molecular weight polymers may prevent reactions from proceeding to completion.

These simulations have not included chain trajectories, as mentioned above, and so they give no insight into the possibility that there is an entanglement contribution to the modulus of elasticity. It is clear, however, that network loops that are speared by chains will never make a significant contribution.[28] When the prepolymer is short so as to favor loop formation, the loops will be too small to circumnavigate the cross section of another chain. When the prepolymer is long enough to do so, the probability for loop formation is reduced so as to decrease the chances for forming such structures.

Application of combinatorial algorithms to cross-linking reactions with spatial constraints on the primary chains provides a basis for understanding the role of intramolecular reactions on network and sol structure. It would be useful to compare the quantitative information obtained by this computer simulation with other experimental data, such as GPC or HPLC analysis of the sol composition, or by measurement of the population of loops.[29]

ACKNOWLEDGMENT

This work was supported by the Department of Energy, contract DE-AT06-81ER10912.

[1]P. J. Flory, *Principles of Polymer Chemistry* (Cornell University, Ithaca, 1962), Chap. 9.
[2]W. H. Stockmayer, J. Chem. Phys. **12**, 125 (1944).
[3]M. Gordon and W. B. Temple, Makromol. Chem. **160**, 263 (1972); W. B. Temple, *ibid.* **160**, 277 (1972).
[4]R. F. T. Stepto, in *Developments in Polymerization-3*, edited by R. N. Haward (Applied Science, Essex, 1982), Chap. 3.
[5]J. M. Hammersley and D. C. Handscomb, *Monte Carlo Methods* (Wiley, New York, 1965).
[6]D. Stauffer, A. Coniglio, and M. Adam, Adv. Polym. Sci. **44**, 103 (1982).
[7]K. Dušek, M. Gordon, and S. B. Ross-Murphy, Macromolecules **11**, 236 (1978).
[8]J. Mikeš and K. Dušek, Macromolecules **15**, 93 (1982).
[9]D. R. Miller and C. W. Macosko, Macromolecules **9**, 206 (1976).
[10]H. L. Frisch, J. M. Hammersley, and D. J. A. Welsh, Phys. Rev. **126**, 949 (1962).
[11]Y.-K. Leung and B. E. Eichinger, Div. Polym. Mater. **48**, 440 (1983); (preprint).
[12]Y.-K. Leung and B. E. Eichinger, in *Characterization of Highly Crosslinked Polymers*, edited by S. S. Labana and R. A. Dickie, ACS Symposium Series (American Chemical Society, Washington, D.C., 1984), Vol. 243, p. 21.
[13]B. E. Eichinger, J. Chem. Phys. **75**, 1964 (1981); B. E. Eichinger and J. E. Martin, *ibid.* **69**, 4595 (1978).
[14]P. J. Flory, *Statistical Mechanics of Chain Molecules* (Interscience, New York, 1969), Chap. 5.
[15]A. Nijenhuis and H. S. Wilf, *Combinatorial Algorithms* (Academic, New York, 1975), Chap. 18.
[16]International Mathematical and Statistical Libraries Inc. (IMSL) program GGUBS and program GGNML.
[17]J. E. Mark, R. R. Rahalkar, and J. L. Sullivan, J. Chem. Phys. **70**, 1794 (1979); J. E. Mark and J. L. Sullivan, *ibid.* **66**, 1006 (1977).
[18]M. Gottlieb, C. W. Macosko, G. S. Benjamin, K. O. Meyers, and E. W. Merrill, Macromolecules **14**, 1039 (1981).
[19]V. A. Vyssotsky, S. B. Gordon, H. L. Frisch, and J. M. Hammersley, Phys. Rev. **123**, 1566 (1961).
[20]Y.-K. Leung and B. E. Eichinger, J. Chem. Phys. **80**, 3886 (1984).
[21]P.-H. Sung, S.-J. Pan, J. E. Mark, V. S. C. Chang, J. E. Lackey, and J. P. Kennedy, Polym. Bull. **9**, 375 (1983).
[22]P. J. Flory, Proc. R. Soc. London, Ser. A **351**, 351 (1976).
[23]F. Harary, *Graph Theory* (Addison-Wesley, Reading, Mass., 1969).
[24]P. J. Flory, Macromolecules **15**, 99 (1982).
[25]J. P. Queslel and J. E. Mark, Adv. Polym. Sci. (to be published).
[26]K. Dušek and V. Vojta, Br. Polym. J. **9**, 164 (1977).
[27]C. W. Macosko and G. S. Benjamin, Pure Appl. Chem. **53**, 1505 (1981).
[28]B. E. Eichinger, in *Elastomers and Rubber Elasticity*, ACS Symposium Series, **193**, 243 (1982).
[29]J. L. Stanford and R. F. T. Stepto, Br. Polym. J. **9**, 124 (1977).